Rev. Int. Contam. Ambie. 39, 523-546, 2023
https://doi.org/10.20937/RICA.54743

URBAN WRF-CHEM EVALUATION OVER A HIGH-ALTITUDE TROPICAL CITY

Evaluación del WRF-Chem urbano sobre una ciudad tropical de alta elevación

José Miguel NOYOLA POBLETE* and José Agustín GARCÍA REYNOSO

Instituto de Ciencias de la Atmósfera y Cambio Climático, Universidad Nacional Autónoma de México, Circuito de la Investigación Científica s/n, Ciudad Universitaria, 04510 Ciudad de México, México.

*Author for correspondence: jose.noyola@atmosfera.unam.mx

(Received: March 2022; accepted: December 2022)

Key words: air quality, ozone, carbon monoxide, LCZ, multi-layer UCM, WRF-Urban, WRF BEP model.

ABSTRACT

Morphology and grid resolution are important aspects that need to be considered in urban modeling applications, since together with buildings they induce a direct effect on wind and dispersion of pollutants over urban areas. In this study, we evaluate high-resolution simulations of a multi-layer urban canopy model (UCM) based on a local climate zone (LCZ) classification coupled to the Weather Research and Forecasting model with Chemistry (WRF-Chem), in the local meteorological conditions and air quality pollutants of a highly urbanized megacity. This modeling system, known as Building Effect Parameterization (BEP) considers the effects of buildings' vertical and horizontal surfaces on the momentum that considerably impacts the lower part of the urban boundary layer (UBL). Simulations of the urbanized model (WRFu) were compared against a Noah land surface model (Noah LSM) with no urban physics (WRF) for the same period. It was observed that the LCZ classification and urban parameterization coupled to the model have a direct influence in meteorological parameters and pollutant concentrations. Urban simulations of temperature and wind speed showed higher sensitivity to initial and boundary conditions, increasing the correlation with observations and reducing the bias error. An important observation is that emissions drive air quality concentrations despite the improvements in local meteorology.

Palabras clave: calidad del aire, ozono, monóxido de carbono, LCZ, UCM multicapa, WRF-Urbano, modelo WRF BEP.

RESUMEN

La morfología y la resolución de celda son aspectos importantes que necesitan considerarse en las aplicaciones de modelación urbana, ya que junto con los edificios inducen un efecto directo sobre el viento y la dispersión de contaminantes en áreas urbanas. En este estudio evaluamos simulaciones de alta resolución de un modelo de dosel urbano (UCM, por su sigla en inglés) multicapa, basado en una clasificación por zonas climáticas locales (LCZ) acoplada al Modelo para la Predicción e Investigación del Clima con Química (WRF-Chem) en las condiciones meteorológicas locales y los contaminantes de calidad del aire de una megaciudad altamente urbanizada. Este sistema de modelación, conocido como parametrización de efecto de construcciones (BEP) toma en cuenta los efectos de las superficies verticales y horizontales de los edificios sobre el momento que impacta considerablemente sobre la parte más baja de la capa límite urbana (UBL). Las simulaciones del modelo urbanizado (WRFu) fueron comparadas contra las simulaciones del modelo de superficie terrestre Noah (Noah LSM) sin física urbana (WRF) para el mismo periodo. Se observó que la clasificación LCZ y la parametrización urbana acoplada al modelo tienen una influencia directa en los parámetros meteorológicos y las concentraciones de contaminantes. Las simulaciones urbanas de temperatura y velocidad del viento mostraron una mayor sensibilidad a las condiciones iniciales y de frontera, incrementando la correlación con las observaciones y reduciendo el error de sesgo. Un aspecto importante encontrado es que las emisiones controlan las concentraciones de calidad del aire a pesar de las mejoras en la meteorología local.

INTRODUCTION

Air quality modeling is a growing interest in both urban and rural areas, particularly in the former due to the high density of population. Between 1950 and 2018 the world's population underwent rapid urbanization, with the urban proportion rising from 30% in 1950 to 55% in 2018. By 2050, the urban fraction of the world's population is projected to reach 68% (UN 2019). For this reason, urban modeling has become an important aspect not only for air quality but also for local meteorology assessments that require a better representation of the physical processes involved in urban environment mesoscale modeling. Thus, the Urban Canopy Model (UCM) with a single layer has been coupled to the Weather Research and Forecasting (WRF) model to improve the description of lower conditions of the urban boundary layer (UBL) and to provide more accurate forecasts for urban regions (Tewari et al. 2007). One key requirement for urban applications is that the WRF accurately represents city morphology influences on wind, temperature, and humidity in the atmospheric boundary layer and their collective influences on the atmospheric mesoscale motions (Chen et al. 2011).

Several urban parameterizations in the WRF have been used and coupled with the Noah Land Surface Model (LSM) (Chen and Dudhia 2001, Kong et al. 2021) through the urban percentage parameter (or urban fraction, F_{urb}), which represents the proportion of impervious surfaces in the WRF sub-grid scale. Noah LSM provides surface-sensible, latent heat fluxes, and surface skin temperature as lower boundary conditions for coupled atmospheric models, whereas UCM provides the fluxes from anthropogenic surfaces. The relevance of urban-scale modeling is not only increasing with WRF but also with different modeling approaches; however, a small number of studies has been conducted in the field of environmental sciences (Wong et al. 2021). A bulk urban parameterization was included in WRF V2 (Chen et al. 2011). Then, the Single-Layer Urban Canopy Model (SLUCM) was developed, adopting infinitely long street canyons parameterized to represent urban geometry, but recognizing the three-dimensional nature of urban surfaces (Chen et al. 2011). Subsequently, the multi-layer Urban Canopy Model known as BEP for Building Effect Parameterization was developed by Martilli et al. (2002). Several modeling studies have been made using different kind of models and parameterizations (Ulpiani 2021). The study of Liao et al. (2014) evaluated diverse urban canopy schemes in the WRF model coupled with chemistry (WRF-Chem), including the SLUCM, the multi-layer UCM (BEP), and the multi-layer urban model with a Building Energy Model (BEM) that includes anthropogenic heat due to air conditioning (BEP + BEM). They determined that wind speed at 10 m decreases when urban canopy schemes are coupled to the model (Liao et al. 2014), which is important for air quality issues.

Several modeling studies have been carried out in the central region of Mexico; however, only a small number report the use of urban parameterizations. Ozone (O_3) production and response under different meteorological conditions was studied in the Mexico City Metropolitan Area (MCMA) during a field campaign in 2003, precising that O_3 production depends on pollutant emissions and meteorological conditions (Lei et al. 2008). Correspondingly, in the MILAGRO field campaign numerous studies were performed in the Mexico City region in order to characterize chemical and physical transformations, and to assess impacts of exported pollutants from urban areas on regional and global air quality, ecosystems and climate. The effects of spatial resolution over trace gases and aerosols suggest that simulations at a 3-km horizontal grid resolution adequately reproduce the overall transport and mixing of trace gases and aerosols downwind of Mexico City, whereas a large grid resolution (such as 75 km) is insufficient to represent both local emissions and the terrain impact on meteorological fields affecting dispersion and transport of trace gases and aerosols and their sub-grid variability (Qian et al. 2010).

Zhang et.al. (2009) assessed meteorological variables and criteria pollutants simulated with the WRF-Chem model against measurements from the Red Automática de Monitoreo Atmosférico (Automatic Air Quality Monitoring Network, RAMA), finding there is a cold bias in temperature surface between 1 and 2 ºC from daytime to nighttime, being probably one of the reasons that the 3-km grid resolution is insufficient to resolve small scale circulations in urban environments and the urban infrastructure effects, which were not included in this work (Zhang et al. 2009). This is supported in the study made by Tie et al. (2010) to illustrate the effects of horizontal spatial resolutions on concentrations of O_3 and its precursors in a mega city, whose results show that model resolution has important effects on calculations of air pollutants dispersion in urban areas and photochemical O_3 production, due to calculated meteorological conditions, spatial distribution of emissions and the non-linearity of photochemical O_3 production (Tie et al. 2010). A previous study found that O_3 concentrations in a city plume are very sensitive to meteorological and ambient chemical conditions, including extra-urban scale transport winds, wind field vertical structure, and mixing processes (Tie et al. 2009); therefore, we can expect that including an urban parameterization and increasing grid resolution in the model could lead to an improve in local meteorology and air quality simulations.

According to Zhang et al. (2009), characterizing the impacts of urban pollutants requires detailed modeling studies. Mexico City's air quality and meteorological forecast (AQFS-CDMX), run by the Secretaría del Medio Ambiente de la Ciudad de México (Mexico City Environment Secretariat, SEDEMA), incorporates such characteristics by connecting a meteorological model (WRF-ARW) and a regional emissions model with the Community Multi-scale Air Quality (CMAQ) chemical transport model and the Noah LSM with single-layer Urban Canopy Model (UCM), in order to estimate the air quality for the next 24 h in the MCMA (SEDEMA 2017) and support the activation and suspension of atmospheric environmental contingencies (SEDEMA 2019). In addition, to characterize Mexico City's urban meteorological conditions, the WRF model was coupled with the multi-layer UCM (BEP) and the WUDAPT level 0 (Martilli et al. 2016), and then configured to run four nested domains of 13.5, 4.5, 1.5, and 0.5-km grid resolutions. A comparison of the urban integration (WRFu) against the traditional (WRF) simulations and observations was made for both dry and wet seasons in 2016, showing that WRFu better captures the influence of the city over changes in temperature, wind speed, and planetary boundary layer (PBL) in comparison with the WRF simulations. WRFu also showed a greater urban heat island effect during daytime and simulations were closer to observations in both seasons (Fernández 2017). A similar study was developed in the city of Barcelona to evaluate the performance of urban schemes integrated in the WRF, including BEP. In average, highest correlations with observations for temperature and wind speed were obtained by BEM in comparison with WRF (Ribeiro et al. 2021).

The multi-layer UCM parameterization has already been implemented for the central region of Mexico; however, there are some gaps that still need to be addressed, such as the implementation of the Chem module in WRFu in order to assess air quality simulations, which is the main purpose of this study. In this work, we describe the implementation of the urban WRF, including a multi-layer urban canopy model (BEP) with chemistry to simulate air quality pollutants. In order to select an optimal configuration for this model, sensitivity assessments were conducted by increasing the grid resolution from 1 m to 0.5 km and by changing the initial and boundary conditions to evaluate the impact over local meteorology. In addition, a comparison between the urban WRF-Chem (WRFu-Chem) and WRF-Chem simulations without urban parameterization and local observations is presented for carbon monoxide and O_3 as model performance evaluation.

MATERIALS AND METHODS

Study area description

The MCMA is defined by the conurbation of 76 municipalities from three entities: 16 of Mexico City (CDMX), 59 of the State of Mexico, and one of the state of Hidalgo (SEDATU 2018). The study area comprises some municipalities of the State of Mexico, Morelos and the entire CDMX, as shown in **figure 1**, where urban and rural regions of the latter, surrounded by urban areas of the State of Mexico (12 M inhabitants), are also displayed. The

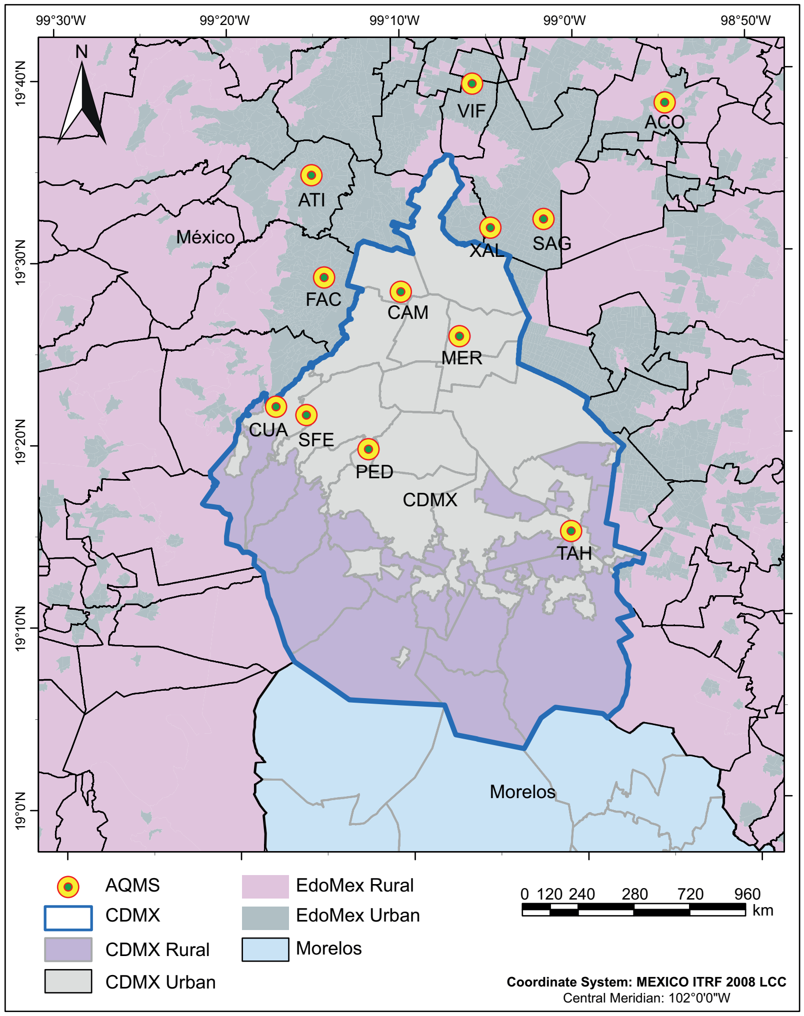

Fig. 1. Map of the study area, including the Mexico City Metropolitan Area (MCMA) delimited by a blue line and the surrounded areas of the states of Mexico and Morelos. Urban and rural areas of the MCMA are also identified in light gray and lilac colors, respectively. Pink and gray regions correspond to rural and urban areas of the State of Mexico, respectively. The blue light zone is the rural area of Morelos. Dots labeled as AQMS relate to the Air Quality Monitoring Stations of the Sistema de Monitoreo Atmosférico (SIMAT) used to evaluate the model performance. Source: INEGI (2018).

CDMX (19.0482-19.5928º N, 99.3649-98.9403º W, with elevations between 2240-3930 masl [INEGI 2022]) has a total population of 8 985 339 inhabitants. It sits in a closed basin surrounded by mountains, with the nearest mountain range located to the southeast, south and west, and the highest mountains found to the east about 40 km from the city center. The study area is displayed in **figure 1**. In 2014, the CDMX annual mean temperature was 17.7 ºC, with an annual mean maximum of 23.8 ºC and a minimum of 11.5 ºC. The mean precipitation for this year was 655.9 mm (CONAGUA 2014).

Air quality observations data

In order to evaluate the model performance, air quality data from the Sistema de Monitoreo Atmosférico (Atmospheric Monitoring System, SIMAT) of Mexico City were used. Criteria pollutants (O_3, SO_2, NO_2, CO, PM_{10}, $PM_{2.5}$, are measured by RAMA in 34 stations throughout the city, and surface meteorological parameters (temperature, relative humidity, wind direction, and wind speed) are measured continuously in 26 different sites of the Red de Meteorología y Radiación Solar (Meteorology and Solar Radiation Network, REDMET). These data are available in hourly average format and can be accessed within the air quality webpage of Mexico City (GCDMX 2019). The air quality monitoring stations (AQMS) used to evaluate the model performance are indicated in **figure 1**. It should be noted that stations Santa Fe (SFE), Cuajimalpa (CUA), and Tlahuac (TAH) are in the edge of the mountain range. On the other hand, Atizapán (ATI), San Agustín (SAG), FES Acatlán (FAC) and Villa de las Flores (VIF) are located in semi-urban regions, mostly surrounded by rural areas, while Acolman (ACO) is located in a rural area. The rest of the AQMS are located in urban areas, as shown in **table I**.

Description of the urban WRF-Chem modeling system

The Weather Research and Forecasting (WRF) model is a next-generation mesoscale numerical weather prediction system designed both for atmospheric research and operational numerical weather predictions (NWP), and is suitable for applications on air quality modeling, among others (Skamarock et al. 2005). The WRF model incorporates several physics options. In this study the BEP model, which is considered the most high-level modeling in WRF for urban applications, has been included (Chen et al. 2011), alongside WRF v. 3.2. The core of the urban WRF-Chem is shown **figure 2**, in which red boxes correspond to the built-in modules in the WRFu-Chem modeling system and the main application. These modules will be described briefly in the following sections.

Building Effect Parameterization (BEP) model

The BEP model comprises a multi-layer UCM developed by Martilli et al. (2002), which allows direct interaction with the PBL and recognizes the 3D nature of urban surfaces considering vertical effects (walls) and horizontal surfaces (streets and roofs) on the momentum (drag-force approach), turbulent kinetic energy (TKE), and potential temperature that substantially impacts the thermodynamic structure of

TABLE I. AIR QUALITY MONITORING STATIONS (AQMS) INCLUDED IN THIS STUDY WITH THEIR LOCATION AND HEIGHT.

Site ID	Latitude	Longitude	Height (m)	Site name	Observations
ACO	19.6355	–98.9120	2198	Acolman	Rural
CUA	19.3653	–99.2917	2704	Cuajimalpa	Urban
FAC	19.4824	–99.2435	2299	FES Acatlán	Semiurban
MER	19.4246	–99.1196	2245	Merced	Urban
PED	19.3251	–99.2041	2326	Pedregal	Urban
SAG	19.5329	–99.0303	2241	San Agustín	Urban
ATI	19.5769	–99.2541	2341	Atizapán de Zaragoza	Semiurban
CAM	19.4684	–99.1698	2233	Camarones	Urban
XAL	19.5259	–99.0824	2160	Xalostoc	Urban
SFE	19.3573	–99.2628	2599	Santa Fe	Semiurban
TAH	19.2464	–99.0105	2297	Tlahuac	Semiurban
VIF	19.6582	–99.0966	2242	Villa de las Flores	Semiurban

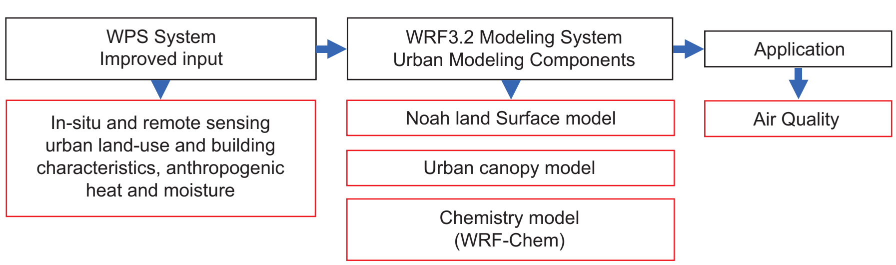

Fig. 2. Overview of the Urban Weather Research and Forecasting with Chemistry (WRFu-Chem) modeling system implemented for this study. It includes urban modeling data-ingestion enhancements in the WRF pre-processor system (WPS), a suite of urban modeling tools in the core physics of WRFV3.2 and its main application. Source: adapted from Chen et al. (2011).

the urban roughness sub-layer, and hence the lower part of the UBL. The BEP scheme is operational with Noah LSM and has been coupled with two turbulence schemes: Bougeault and Lacarrère (1989) and Mellor-Yamada-Janjić (Janjić 1994), making it able to simulate some of the most observed features in urban atmosphere, such as the nocturnal urban heat island (UHI) and the elevated inversion layer above the city (Chen et al. 2011).

A key requirement for urban applications in the WRF is to accurately capture influences of cities on wind, temperature, and humidity in the atmospheric boundary layer, as well as their collective influences on the atmospheric mesoscale motions. Chen et al. (2011) established that to take full advantage of BEP, it is necessary to have high vertical resolution close to the ground. In order to consider influences of buildings over meteorological parameters we use 51 vertical levels in this application with a height of about 20 m for the first layer and a 0.5-km grid resolution for the finest domain.

Urban land use

To run the multi-layer urban canopy model version of BEP embedded in WRFV3.2, data from the World Urban Database and Access Portal Tools (WUDAPT) level 0 was used. WUDAPT level 0 is based on the LCZ classification scheme (Steward and Oke 2012, Stewart et al. 2014). **Figure 3** shows a summary of the methodology followed for implementing the WRFu-Chem modeling system (Martilli et al. 2016).

To use WUDAPT level 0 as input for BEP in WRFV3.2 it is necessary to follow up the following steps:

- Extension of the number of urban classes from 3 to 10 as stated in Steward and Oke (2012).
- Using the LCZ map created by WUDAPT level 0 as a foundation, we conducted an update of the land use field (LU_INDEX).
- Modification of the URBPARM.TBL table to define supplementary parameters such as urban fraction, building heights, heat capacity, etc., for each urban class (Martilli et al. 2016).

Various studies have demonstrated that changes in land use impact meteorological parameters and pollutants, and these changes vary according to the urban canopy schemes used (Liao et al. 2014). In this study, the default USGS land use configuration of LANDUSE.TBL, structured in 24 categories, was used in WPS. Then, urban categories were extended to 10 different categories according to the method used by Martilli et al. (2016) in WUDAPT level 0 based on the LCZ classification. In this way, the new categories of urban classification correspond to the categories from item 31 to 40.

WRF-Chem module

The WRF-Chem model simulates emission, transport, mixing, and chemical transformation of trace gases and aerosols simultaneously with meteorology. It is used for investigation of regional-scale

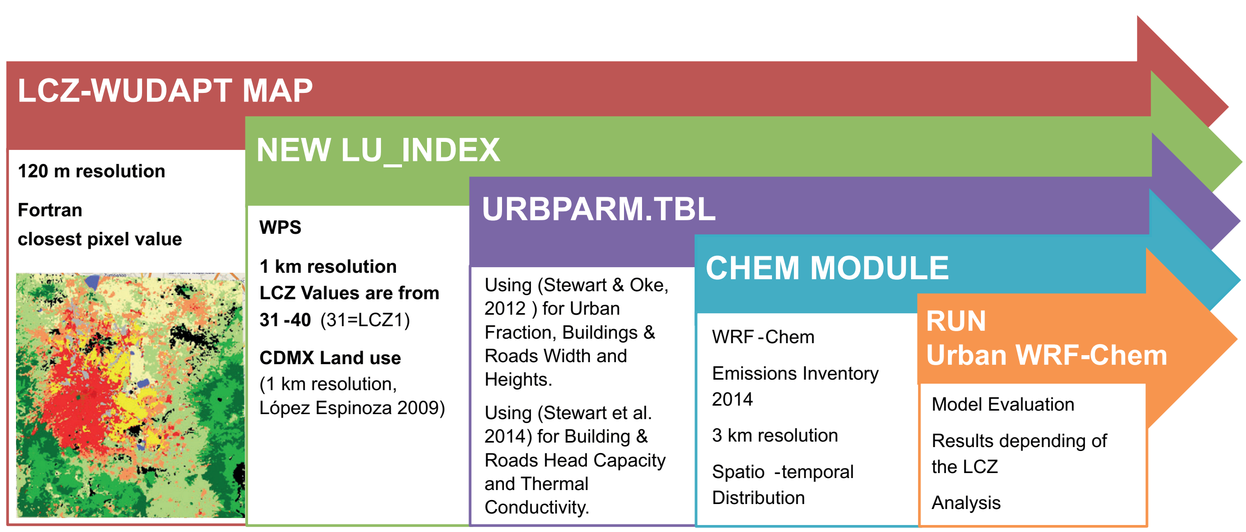

Fig. 3. Scheme of the methodology for using the World Urban Database and Access Portal Tools (WUDAPT) level 0 to implement the multi-layer Building Effect Parameterization (BEP) with the Urban Weather Research and Forecasting with Chemistry (WRFu-Chem) modeling system. Source: adapted from Martilli et al. (2016).

air quality, field program analysis, and cloud-scale interactions between clouds and chemistry (Grell et al. 2005, NCAR 2020a). WRF-Chem is coupled with several modules for working with anthropogenic and biogenic emissions, allowing several choices for gas-phase chemical mechanisms like RADM2, RACM, SAPRC99, among others, and also for photolysis and aerosol schemes (Peckham 2010). Detailed information about the WRF-chem model is presented in Grell et al.(2005) and Fast et al. (2006).

Emissions inventory

The emissions used for chemical simulation corresponds to the National Emissions Inventory, which is considered a hybrid inventory since it consists of different years emissions as follows: 2013 for point source emissions; 2014 for source area emissions; and 2015 for mobile emissions. The Inventory only comprises the emissions of Mexico. Regarding time distribution it considers hourly emissions data, as well as UTM and latitude-longitude in degrees coordinates (INECC 2017). The emissions information contains organic and inorganic species according to RADM2 mechanism used for modeling the atmospheric chemistry (Stockwell et al. 1990). To produce emission input data for WRFu-Chem simulations, these emissions were interpolated using a mass conservative method[1] into the three domains throughout the initial condition files wrfinput_d01, wrfinput_d02 and wrfinput_d03 generated by the real.exe program. For details on the spatial and temporal distribution and speciation refers to (García-Reynoso et al. 2018).

WRFu-Chem model configuration

Meteorological input data

The meteorological input data used as boundary conditions to initialize the urban modeling system through the WRF Preprocessing System (WPS) are the National Center for Environmental Prediction (NCEP) final (FNL) Operational Global Analysis data, with 1-degree by 1-degree spatial resolution and prepared operationally every six hours of temporal resolution (NCAR 2020) and the NCEP North American Mesoscale (NAM) Forecast System data with 12 km spatial resolution every 6 hours (NCAR 2020).

Study case

During February 19th 2014 to February 27th 2014, measurements of O_3, PM_{10} and $PM_{2.5}$ with the nearest monitoring sites (CUA, SFE) were compared, showing a high correlation in tendency of these pollutants (Noyola 2014). The WRFu-Chem modeling system was set up to simulate this case. This modeling system will be helpful to study further episodes of high pollutant concentrations in the region, for network monitoring design and also to evaluate spatial representativeness of air quality monitoring stations that will be presented in a separate study. The simulations run continuously over 150 hours, starting from February-20-2014 00:00:00 UTC and ending at February-26-2014 06:00:00 UTC. Only the simulations from days 21-00:00:00 to 25-23:00:00 of local time (UTC-06:00) were used to evaluate the model performance against measurements of the monitoring stations of the RAMA.

Domain configuration

For this study, three nested domains were set up for simulations. The domains are shown in **figure 4** as follows: the coarse domain (d01) has 79 x 79 cells with a 4.5 km x 4.5 km grid resolution; the second domain (d02) has 1.5 km x 1.5 km grid resolution;

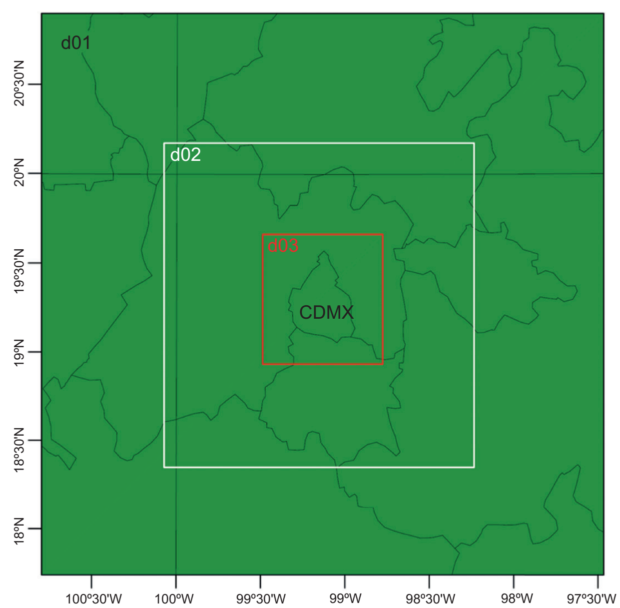

Fig. 4. Domain configuration. Three nested domains were configured for simulations. The coarse domain has 6241 cells with a 4.5 x 4.5 km grid resolution; the second domain has a 1.5 x 1.5 km grid resolution, and the third and finest domain has a 0.5 x 0.5 km grid resolution, covering a total of 6153 km^2, including the entire Mexico City.

[1]Obtained from https://github.com/JoseAgustin/interpola

and the third and the finest domain (d03) has 151 x 163 cells with 0.5 km x 0.5 km grid resolution that comprise the entire CDMX and part of Mexico State where monitoring stations are also installed and used for the model evaluation. The map in **figure 1** illustrates the finest domain d03 in detail. Due to computational reasons, usually the model resolution cannot be higher enough to consider the effects induced by buildings on wind and dispersion and thus, the turbulent flow around the urban obstacles cannot be resolved explicitly. In order to consider the atmospheric processes inside the Urban Canopy Layer induced by the urban morphology, a high resolution of 0.5 km was set for the finest domain (Santiago and Martilli 2010).

Physics

In order to simulate the PBL effects in WRFu-Chem model over wind speed and temperature, the option bl_pbl_physics = 8 was used. This PBL scheme was designed for using with BEP urban model integrated in WRF model. To select between Noah Land Surface Model with no urban physics (WRF) and the multi-layer urban canopy model urban parameterization embedded in BEP (WRFu), the parameterizations described in **table II** were used. Additional physic parameterization configured for running the model is described in **table III**.

TABLE II. SIMULATION SCENARIOS WITH DIFFERENT URBAN CANOPIES. NOAH LAND SURFACE MODEL (LSM) WITH NO URBAN PHYSICS (WRF) AND THE MULTI-LAYER URBAN CANOPY MODEL (UCM) PARAMETERIZATION (WRFu) EMBEDDED IN BUILDING EFFECT PARAMETERIZATION (BEP) MODEL.

Scenario	Parameterization	Observation
WRF	sf_urban_physics = 0	No urban physics is used
WRFu	sf_urban_physics = 2	BEP model is used

RESULTS AND DISCUSSION

In order to identify the best configuration for WRFu-Chem, six different experiments were conducted, including two with input data for initial and

TABLE III. URBAN WEATHER RESEARCH AND FORECASTING WITH CHEMISTRY (WRFu-Chem) PHYSICS PARAMETERIZATION USED FOR SIMULATIONS*.

Physics variable name	Option	Scheme description
mp_physics	4	WRF Single-Moment 5-class scheme: A simple efficient scheme with ice and snow processes suitable for mesoscale grid sizes. Allows for mixed-phase processes and super-cooled water.
ra_lw_physics	1	RRTM scheme: Rapid Radiative Transfer Model. An accurate scheme using lookup tables for efficiency. Accounts for multiple bands, trace gases and microphysics species (Mlawer et al. 1997).
ra_sw_physics	2	Goddard shortwave: Two-stream multi-band scheme with ozone from climatology and cloud effects.
sf_sfclay_physics	2	Eta similarity: Used in Eta model. Based in Monin-Obukhov with Zilitinkevich thermal roughness length and standard similarity functions from look-up tables.
sf_surface_physics	2	Noah Land Surface Model: Unified NCEP/NCAR/AFWA scheme with soil temperature and moisture in four layers, fractional snow cover and frozen soil physics.
bl_pbl_physics	8	BouLac: Bougeault-Lacarrère PBL. A TKE-prediction option (Bougeault and Lacarrère 1989)
sf_urban_physics	0	Noah Land Surface Model: Unified NCEP/NCAR/AFWA scheme with soil temperature and moisture in four layers, fractional snow cover and frozen soil physics. No urban physics.
	2	BEP: Building Environment Parameterization: Multi-layer urban canopy model that allows for buildings higher than the lowest model levels.
cu_physics	5	Grell 3d ensemble cumulus scheme. Scheme for higher resolution domains allowing for subsidence in neighboring columns.

*For the planetary boundary layer scheme (BL_PBL_PHYSICS), option 8 (Bougeault-Lacarrère) designed to be used with Building Effect Parameterization (BEP) was selected.

boundary conditions, changes in grid resolution with two and three nested domains, and urban physics parameterization. The results obtained are presented in this section.

Sensitivity to initial boundary conditions

The experiments configured to assess the sensitivity of the system to initial boundary conditions are described in **table IV**.

Temperature

To evaluate the initial boundary conditions impact on local weather, NCEP FNL (NCAR 2020b) and NAM (NCAR 2020c) input data were used for the same configuration of WRF and WRFu. **Figure 5** shows a time series of 2-m temperature simulations with WRF and WRFu using NAM and FNL data, and their comparison with observations (in black) of different monitoring sites. The WRF model underestimates

TABLE IV. EXPERIMENTS CONFIGURED TO EVALUATE THE SENSITIVITY OF SIMULATIONS TO INITIAL BOUNDARY CONDITIONS: FINAL (FNL) OPERATIONAL GLOBAL ANALYSIS AND NORTH AMERICAN MESOSCALE (NAM) FORECAST SYSTEM DATA*.

No.	Experiment	Grid Resolution	Domains	Sf_urban _physics	Initial and Boundary conditions
1	WRF _ fnl	0.5 km	3	0	FNL
2	WRFu_fnl			2	
3	WRF _ nam			0	NAM
4	WRFu_nam			2	

*All experiments have three domains for simulation and a 0.5 × 0.5 km grid resolution for the finest domain (d03). Urban surface (sf_urban_physics) option is switched between 0 and 2 to select the Noah Land Surface Model (LSM) with no urban physics (WRF) and the Multi-Layer Urban Canopy Model (WRFU) with Building Effect Parameterization (BEP), respectively.

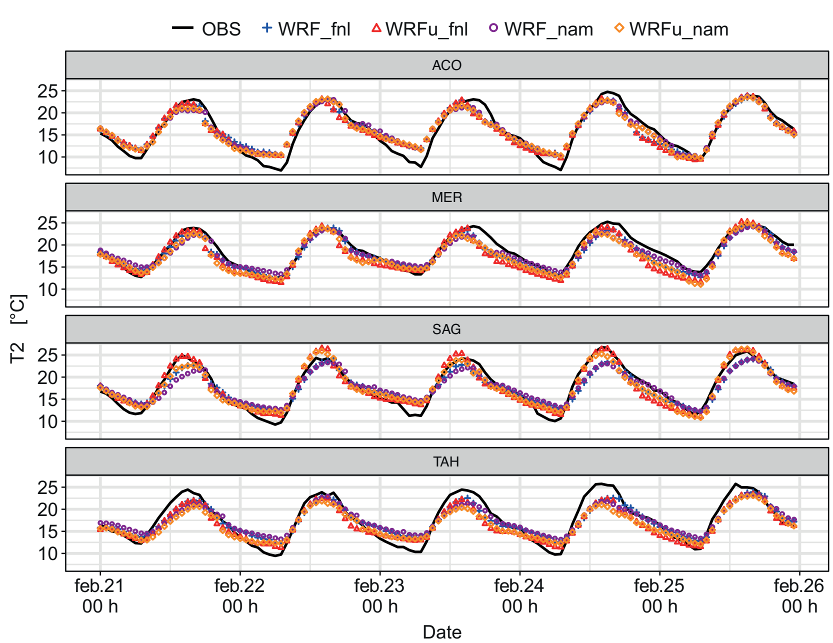

Fig. 5. Comparison of time series in local time (GMT–06:00) of 2-m temperature (T2) observations for different monitoring stations against Weather Research and Forecasting (WRF) and Urban Weather Research and Forecasting (WRFu) simulations, using the North American Mesoscale (NAM) forecast system and final (FNL) Operational Global Analysis data.

high values of observed temperature; in contrast, WRFu simulations are close to observed high values in most of the stations. Nonetheless, in rural areas (ACO) and in zones with low or moderate urbanization (such as FAC, PED, SFE, and TAH) temperature observations tend to be lower than in urban areas. In these cases, both WRF and WRFu fail to reproduce the lowest observed values, though WRFu is more accurate (**Fig. 5**). It means that urban parameterization enhances simulations, increasing the reproducibility of observations; however, a better LCZ classification is needed in the WRFu model to improve local weather simulations in these zones.

To illustrate the differences between NAM and FLN input data in temperature simulations, a statistical comparison for nine sites was made. Bias variability is reduced when using urban parameterization against no urban physic simulations. Also, a reduction of bias error was observed when using NCEP FNL data in both WRF and WRFu in comparison with NAM data. **Table V** shows the verification measures of simulations made with WRF, when no urban physics is used. In this case, 2-m temperature simulations showed a bias error from –0.87 to 0.3 ºC for NAM input data, while for FNL input data the bias error was from –0.95 to 0.21 ºC. The bias error for WRFu simulations (**Table VI**) was from –1.24 to 0.60 ºC for NAM data whereas for simulations with FNL data it was from –1.30 to 0.47 ºC. (In **tables V-VIII** and **XII-XIII** numbers in bold denote minimum and maximum values for each variable).

High correlation values were obtained in temperature for all simulations. WRF correlations were between 0.89 and 0.97 with a variability of 0.08, whereas correlations in WRFu simulations were from 0.92 to 0.96 with a variability of 0.04, which means a reduction between sites. In this situation, WRFu simulations with NAM and FNL data are very similar. In addition, the RMSE is reduced in most sites when WRFu is used and the variability from WRF to WRFu is also reduced in 49% for NAM and 55% for FNL data. A graphical comparison of these metrics is shown in the Taylor Diagram on **figure 6**, where results of WRFu simulations are closer to the observed values. The index of agreement (I_a) also presented higher values, between 0.86 and 0.97 for WRF and above 0.91 for WRFu. In this last situation, the I_a variability is 0.06 for NAM and 0.04 for FNL, which shows in general better results for temperature.

Wind speed

Wind speed simulations with WRF and WRFu underestimate observations; however, a lower bias error for each site is observed when NCEP FNL data are used as initial boundary conditions. The bias error for WRF simulations was from –0.95 to –0.08 m/s for NAM data and from –0.78 to –0.02 m/s for FNL data, as shown in **table VII**.

On the other hand, the bias error for simulations with urban parameterization (WRFu) and NAM data was from –0.70 to –0.04 m/s, whereas for WRFu with FNL data it was from –0.52 to 0.25 m/s (**Table VIII**).

TABLE V. VERIFICATION MEASURES OF THE TWO-METER TEMPERATURE (T2) BIAS ERROR: ROOT MEAN SQUARE ERROR (RMSE), CORRELATION COEFFICIENT AND INDEX OF AGREEMENT (I_a) FOR DIFFERENT SITES WITH THE WEATHER RESEARCH AND FORECASTING (WRF) MODEL USING THE NORTH AMERICAN MESOSCALE (NAM) FORECAST SYSTEM AND FINAL (FNL) OPERATIONAL GLOBAL ANALYSIS DATA.

T2 WRF Site	BIAS (ºC)		RMSE (ºC)		Correlation		I_a	
	NAM	FNL	NAM	FNL	NAM	FNL	NAM	FNL
ACO	**0.30**	**0.21**	1.71	1.83	0.96	0.95	**0.96**	0.96
CUA	**–0.87**	**–0.95**	2.28	2.06	0.91	0.92	0.88	0.91
FAC	–0.50	–0.71	**3.24**	**2.91**	0.92	0.94	**0.86**	**0.90**
MER	–0.61	–0.83	**1.42**	**1.36**	0.96	0.96	**0.96**	0.96
PED	0.05	–0.19	2.60	2.29	0.90	0.91	0.88	0.92
SAG	–0.11	–0.20	2.03	1.78	0.95	0.96	0.93	0.95
SFE	–0.64	–0.77	2.30	2.16	**0.89**	0.90	0.89	0.91
TAH	0.02	–0.18	2.31	1.97	0.95	0.95	0.91	0.94
VIF	0.03	–0.13	1.71	1.51	0.96	**0.97**	0.95	**0.97**

TABLE VI. VERIFICATION MEASURES OF THE TWO-METER TEMPERATURE (T2) BIAS ERROR: ROOT MEAN SQUARE ERROR (RMSE), CORRELATION COEFFICIENT AND INDEX OF AGREEMENT (I_a) FOR DIFFERENT SITES WITH THE URBAN WEATHER RESEARCH AND FORECASTING (WRFu) MODEL USING THE NORTH AMERICAN MESOSCALE (NAM) FORECAST SYSTEM AND FINAL (FNL) OPERATIONAL GLOBAL ANALYSIS DATA.

T2 WRFu	BIAS (ºC)		RMSE (ºC)		Correlation		I_a	
Site	NAM	FNL	NAM	FNL	NAM	FNL	NAM	FNL
ACO	0.11	–0.01	1.80	1.89	0.95	0.94	0.96	0.96
CUA	0.11	0.14	1.63	1.50	0.93	0.93	0.95	0.96
FAC	–0.37	–0.43	**2.38**	**2.12**	0.94	0.95	0.94	0.96
MER	**–1.24**	**–1.30**	1.79	1.95	0.94	0.93	0.94	**0.94**
PED	0.41	0.29	1.83	1.59	0.94	0.95	0.95	0.97
SAG	–0.04	0.04	**1.45**	**1.42**	0.95	**0.96**	**0.97**	**0.98**
SFE	–0.01	0.01	1.75	1.69	**0.92**	**0.92**	0.94	0.95
TAH	–1.03	–1.02	2.37	2.02	0.95	**0.96**	**0.91**	**0.94**
VIF	**0.60**	**0.47**	1.92	1.97	**0.92**	**0.92**	0.96	0.96

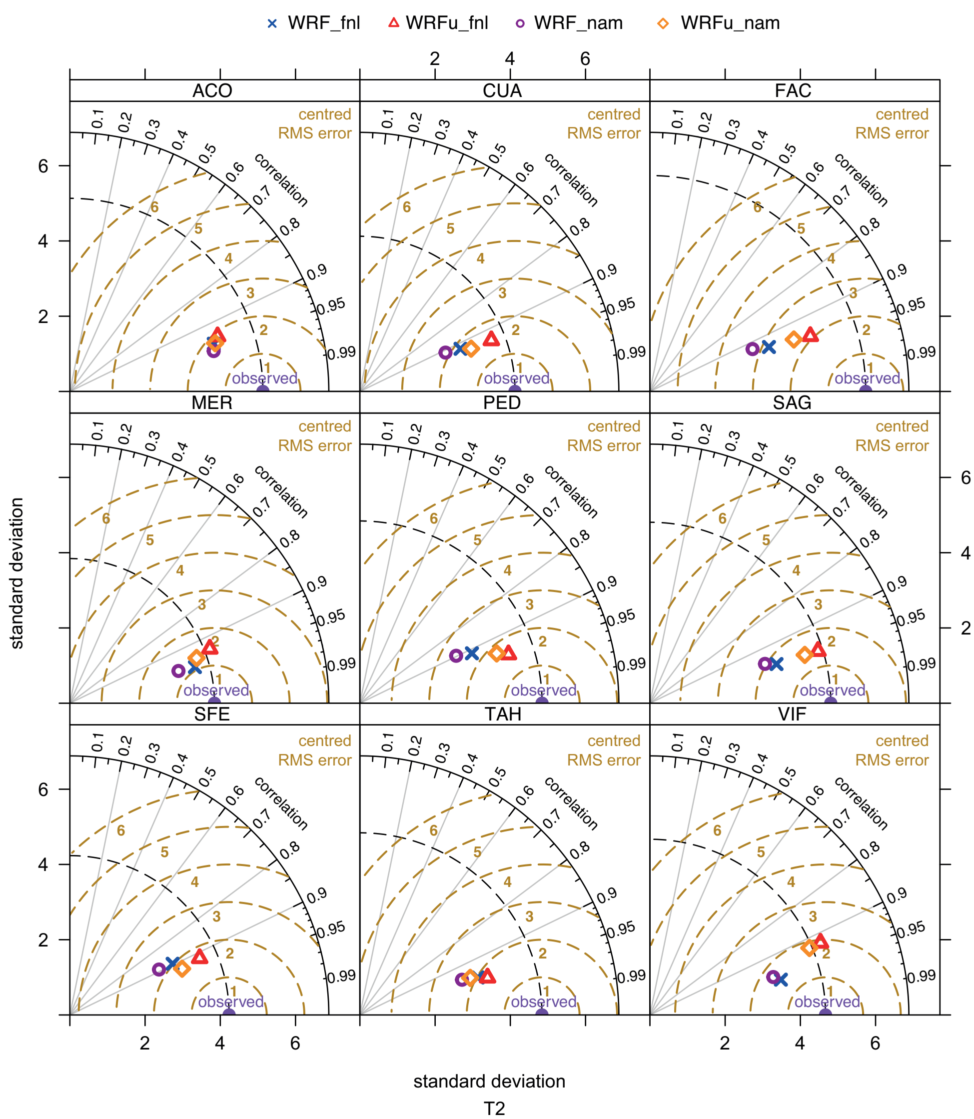

Fig. 6. Two-meter temperature (T2) Taylor diagram of different sites for Weather Research and Forecasting (WRF) and Urban Weather Research and Forecasting (WRFu) simulations with North American Mesoscale (NAM) forecast system and final (FNL) Operational Global Analysis data.

TABLE VII. VERIFICATION MEASURES OF THE WIND SPEED (WS) BIAS ERROR: ROOT MEAN SQUARE ERROR (RMSE), CORRELATION COEFFICIENT AND INDEX OF AGREEMENT (I_a) FOR DIFFERENT SITES WITH THE WEATHER RESEARCH AND FORECASTING (WRF) MODEL USING THE NORTH AMERICAN MESOSCALE (NAM) FORECAST SYSTEM AND FINAL (FNL) OPERATIONAL GLOBAL ANALYSIS DATA.

WRF Site	BIAS (m/s)		RMSE (m/s)		Correlation		I_a	
	NAM	FNL	NAM	FNL	NAM	FNL	NAM	FNL
ACO	**–0.08**	**–0.02**	**1.45**	**1.56**	0.41	0.45	0.61	0.62
CUA	–0.45	–0.27	0.97	**0.97**	0.25	**0.29**	0.5	**0.52**
FAC	–0.53	–0.45	1.12	1.25	0.5	0.42	0.67	0.63
MER	–0.77	–0.6	1.21	1.22	0.54	0.59	0.61	0.65
PED	–0.82	–0.76	1.16	1.19	0.45	0.46	0.53	0.55
SAG	–0.15	–0.02	**0.95**	1.03	**0.72**	**0.7**	**0.78**	**0.76**
SFE	**–0.95**	**–0.78**	1.33	1.23	**0.24**	0.38	**0.44**	0.53
TAH	–0.81	–0.59	1.42	1.36	0.35	0.34	0.56	0.57
VIF	–0.56	–0.39	1.21	1.16	0.34	0.39	0.58	0.61

The maximum bias errors for all simulations were in the Santa Fe (SFE) site, which is in the mountain range side.

A wind-speed Taylor diagram for different sites is shown in **figure 7**. The WRF and WRFu simulations with NAM and FNL initial boundary conditions are graphically and statistically compared. WRFu simulations exhibited greater correlation and lower RMSE than WRF simulations in the stations compared. Furthermore, the index of agreement was also computed and higher values were observed for WRFu simulations compared to WRF. Correlation variability for WRF was 0.48 for NAM and 0.42 for FNL data. For WRFu, the variability of correlation was 0.32 for NAM and 0.38 for FNL data. Variability of RMSE for WRF was 0.50 m/s for NAM data and 0.59 m/s for FNL, whereas variability of RMSE for NAM and FNL simulations with WRFu was 0.68 and 0.79 m/s, respectively. The relatively large variability in RMSE is likely attributed to variations in urban

TABLE VIII. VERIFICATION MEASURES OF THE WIND SPEED (WS) BIAS ERROR: ROOT MEAN SQUARE ERROR (RMSE), CORRELATION COEFFICIENT AND INDEX OF AGREEMENT (I_a) FOR DIFFERENT SITES WITH THE URBAN WEATHER RESEARCH AND FORECASTING (WRFu) MODEL USING THE NORTH AMERICAN MESOSCALE (NAM) FORECAST SYSTEM AND FINAL (FNL) OPERATIONAL GLOBAL ANALYSIS DATA. GLOBAL ANALYSIS DATA.

WRFu Site	BIAS (m/s)		RMSE (m/s)		Correlation		I_a	
	NAM	FNL	NAM	FNL	NAM	FNL	NAM	FNL
ACO	–0.13	**0.25**	**1.49**	**1.66**	0.41	0.43	0.6	0.59
CUA	–0.29	–0.13	0.82	0.89	0.52	0.43	0.65	0.6
FAC	–0.31	–0.24	**0.81**	**0.87**	0.66	0.61	0.78	0.77
MER	–0.6	–0.42	1.07	1.09	0.6	0.65	0.68	0.71
PED	–0.53	–0.49	0.9	0.9	0.58	0.61	0.66	0.68
SAG	**–0.04**	0.07	0.82	0.89	**0.67**	**0.68**	**0.8**	**0.78**
SFE	**–0.7**	**–0.52**	1.22	1.22	**0.35**	**0.3**	**0.52**	**0.51**
TAH	–0.66	–0.29	1.26	1.2	0.49	0.46	0.66	0.67
VIF	–0.23	–0.2	0.9	0.88	0.49	0.54	0.71	0.72

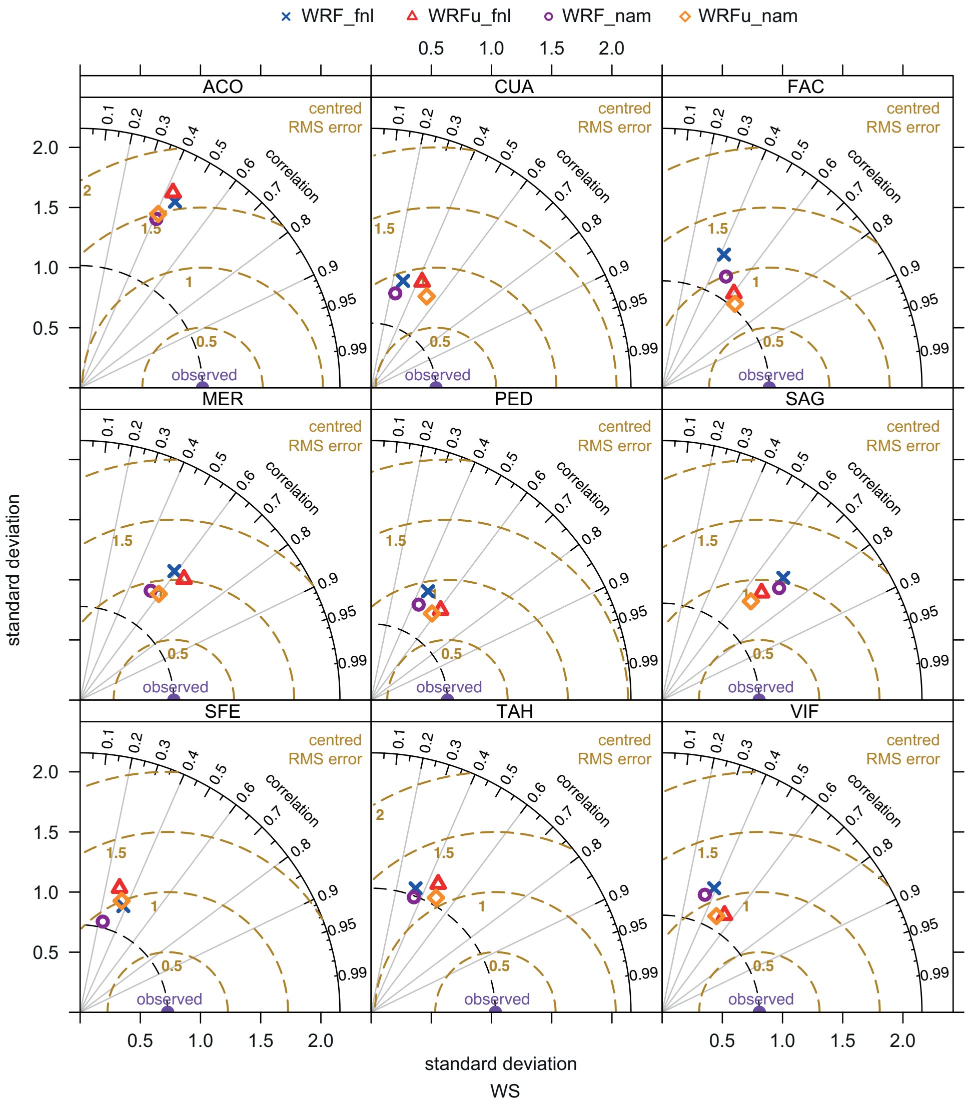

Fig. 7. Taylor diagram of wind speed (WS) for different sites. The Weather Research and Forecasting (WRF) and Urban Weather Research and Forecasting (WRFu) simulations with North American Mesoscale (NAM) forecast system and final (FNL) Operational Global Analysis data are graphically and statistically compared to a reference point in the *X* axis which corresponds to the observation site.

classification as perceived by the WRFu model at each individual station and variations in measurement height.

The previous results suggest that the WRFu model improves simulations of local weather conditions using either NAM or FNL data. In general, when using FNL data in WRFu simulations the bias error is reduced in most sites where the model is compared against observations. In this way and considering the limitations of geographical coverage of NAM data, we decided to use FNL data for the next simulations.

Influence of grid resolution

We evaluated the spatial resolution influence of the model over the study area. For this, four experiments were configured as described in **table IX**. The experiments with ID 1 and 2 have three domains with a grid resolution of 0.5 by 0.5 km for the finest domain (d03); and experiments 3 and 4 have two domains and 1 by 1 km grid resolution for the finest domain (d02). All experiments were run using NCEP FNL input data. The flag sf_urban_physics = 0 was set in order to select between Noah LSF with

TABLE IX. EXPERIMENTS CONFIGURED FOR EVALUATING THE SPATIAL RESOLUTION INFLUENCE OVER LOCAL WEATHER BY USING FINAL (FNL) OPERATIONAL GLOBAL ANALYSIS DATA*.

No.	Run Experiment	Spatial Resolution	Domains	sf_urban_physics	Initial and Boundary conditions
1	WRF - 0.5 km	0.5 km	3	0	FNL
2	WRFu-0.5 km	0.5 km	3	2	
3	WRF - 1 km	1 km	2	0	
4	WRFu-1 km	1 km	2	2	

*Experiments 1 and 2 have three domains for simulation and a 0.5 × 0.5 km grid resolution for the finest domain (d03). Experiments 3 and 4 have two domains for simulation and a 1 × 1 km grid resolution for the finest domain (d02). Urban surface (sf_urban_physics) option is switched between 0 and 2 to select the Noah Land Surface Model (LSM) with no urban physics (WRF) and the Multi-Layer Urban Canopy Model (WRFU) with Building Effect Parameterization (BEP), respectively.

no urban physics (WRF), while sf_urban_physics = 2 was set for using the multi-layer urban canopy model BEP (WRFu).

In **figure 8** a diurnal variation of 2 m temperature observations and simulations of 1 and 0.5 km spatial resolution are shown. It is observed that WRF simulations tend to underestimate high values of temperature, whereas simulations with WRFu increase temperature, reaching high observed values; however, simulations at 1-km resolution overestimate the observations.

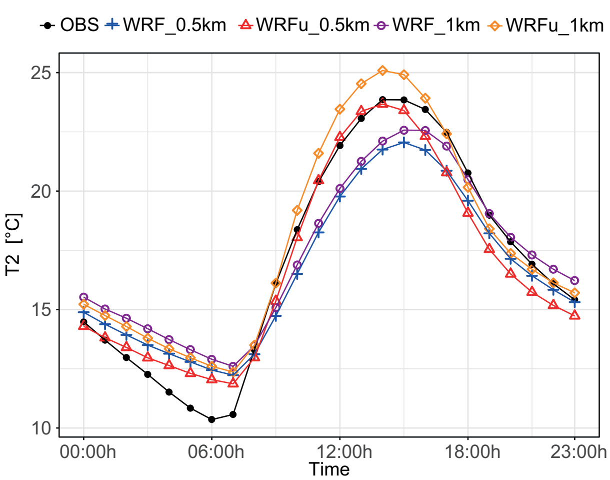

Fig. 8. Diurnal variation of 2-m temperature (T2) for observations in black and simulations of 1 and 0.5 km spatial resolution. While Weather Research and Forecasting (WRF) simulations with no urban physics underestimate high values of observations, Urban Weather Research and Forecasting (WRFu) simulations with urban parameterization reach higher values similar to observations. However, the model output of 1-km resolution overestimate observations, having better results when the resolution increases to 0.5 km.

A reduction in bias variability is observed for both WRF and WRFu simulations when grid resolution is increased from 1 to 0.5 km, as observed in **table X**. Variability for WRF simulations is 1.9 and 1.2 ºC for 1 and 0.5 km, respectively, and 2.6 and 1.8 ºC for 1 and 0.5 km, respectively, in the case of WRFu simulations, which correspond to a bias reduction of 39 and 33%, respectively. Even though RMSE has relatively high values, variability was also reduced about 17 and 39% for WRF and WRFu, respectively, when grid resolution was increased from 1 to 0.5 km. In terms of correlation and index of agreement, similar values were obtained, resulting in values above 0.9, but regarding urban parameterization the observed WRFu variability is lower. The correlation coefficient is lower in WRFu because in some stations (MER, SAG) temperature from WRFu is higher than WRF during early hours and lower during afternoon hours, which indicates that the heat capacity used in those areas has to be reviewed.

Wind speed simulations generally have lower values than observations; however, observed peak values are overestimated in all experiments. Higher peak values were obtained in simulations with 1-km grids, whereas simulations with 0.5-km grid resolutions are closer to the maximum value of observations, causing a 18% reduction of in WRFu bias variability and 8% in WRF. RMSE variability is greater in 0.5 km than 1 km simulations; nonetheless, specific results by site show that WRFu simulations have lower RMSE values than WRF. On the contrary, correlation and index of agreement are generally greater in WRFu than in WRF. The maximum and minimum values of nine sites compared in the experiments are shown in **table XI**.

In conclusion, increasing the resolution in simulations has a positive impact in model performance

TABLE X. VERIFICATION MEASURES FOR THE TWO-METER TEMPERATURE (T2) BIAS ERROR REGARDING 1 AND 0.5 km GRID RESOLUTION EXPERIMENTS: ROOT MEAN SQUARE ERROR (RMSE), CORRELATION COEFFICIENT AND INDEX OF AGREEMENT (I_a)*.

No.	Run experiment	BIAS (ºC)		RMSE (ºC)		Correlation		I_a	
		Max	Min	Max	Min	Max	Min	Max	Min
1	WRF-0.5 km	0.22	–0.95	2.91	1.36	0.97	0.90	0.97	0.90
2	WRFu-0.5 km	0.47	–1.30	2.12	1.42	0.96	0.92	0.98	0.94
3	WRF-1 km	1.50	–0.39	2.81	0.93	0.98	0.90	0.98	0.90
4	WRFu-1 km	1.93	–0.71	2.52	1.37	0.97	0.92	0.98	0.94

*Values correspond only to the maximum and minimum obtained from the nine sites evaluated.

since bias and RMSE are reduced and the correlation coefficient and index of agreement increase. On the other hand, simulations of urban parameterization with WRFu + BEP show a better performance in 2-m temperature (T2) and wind speed. Thus, increasing resolution and including urban details in the WRFu model gives a better approach to observations; nevertheless, an improved definition of the LCZ classification must be included in order to increase the WRFu model performance and reduce bias variability, which deserves further investigation.

Effects of urban parameterization on air quality

Experiments 1 and 2 of **table IX** were used to evaluate the effects of urban parameterization on air quality modeling. Experiment 1 corresponds to WRF simulations without urban parameterization and experiment 2 to WRFu, including BEP. These simulations were run at a 0.5-km grid resolution to better capture influences of local meteorology and urban canopy on air quality. In this study, results of a primary pollutant and tracer, carbon monoxide, and a secondary photochemical pollutant, O_3, are presented.

Ozone

Time series of O_3 observations at different sites are shown in **figure 9**, alongside their comparison with WRF and WRFu simulations. In both cases the temporal profile is well simulated; however, WRFu has slightly lower values than WRF. The simulations consistently underestimate peak observed values during daylight at all sites. This is primarily because it is the first time that a high-resolution emissions inventory is used, and improved meteorology data are employed, which produces a change in ambient concentrations of primary pollutants such as carbon monoxide (CO) and nitric oxide (NO). An increase in CO indicates an increment in NO concentrations, then a titration of O_3 occurs in the WRFu and a lower peak is obtained. A sensitivity analysis for nitrogen oxides (NO_x) and volatile organic

TABLE XI. VERIFICATION MEASURES FOR THE WIND SPEED (WS) BIAS ERROR REGARDING 1 AND 0.5 km GRID RESOLUTION EXPERIMENTS: ROOT MEAN SQUARE ERROR (RMSE), CORRELATION COEFFICIENT AND INDEX OF AGREEMENT (I_a)*.

No.	Run Experiment	BIAS (m/s)		RMSE (m/s)		Correlation		I_a	
		Max	Min	Max	Min	Max	Min	Max	Min
1	WRF-0.5 km	–0.02	–0.78	1.56	0.97	0.70	0.29	0.76	0.52
2	WRFu-0.5 km	0.25	–0.52	1.66	0.87	0.68	0.30	0.78	0.51
3	WRF-1 km	–0.02	–0.86	1.50	1.12	0.60	0.31	0.75	0.50
4	WRFu-1 km	0.24	–0.71	1.36	0.89	0.68	0.28	0.82	0.48

*Values correspond only to the maximum and minimum obtained from the nine sites evaluated.

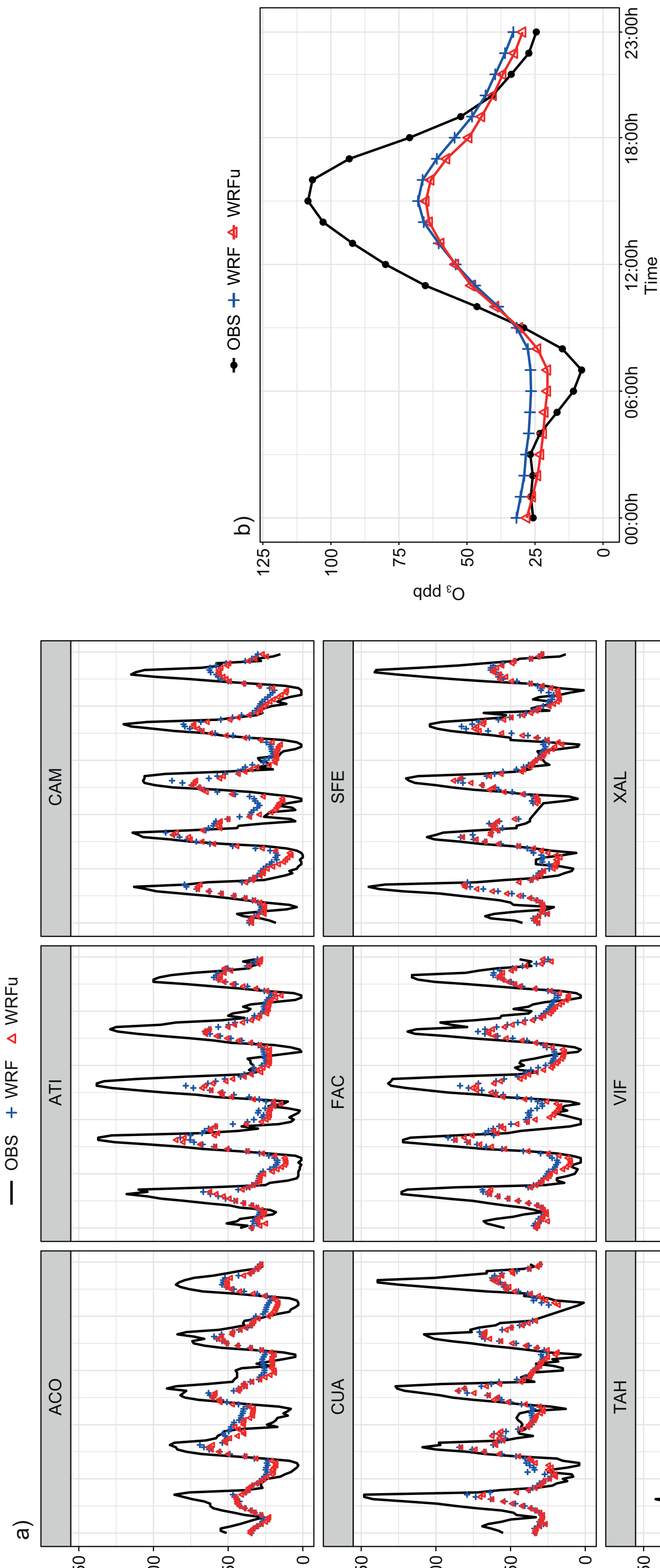

Fig. 9. Ozone (O_3) time series comparing (a) observations of different monitoring station in Mexico City with simulations, and (b) the diurnal variation including all observations and simulations. Peak values are underestimated in both Weather Research and Forecasting (WRF) and Urban Weather Research and Forecasting (WRFu) mdels, probably due to an increase in nitric oxide (NO) concentrations that may titrate O_3.

compounds (VOC) emissions is required to improve O_3 concentrations and it deserves more research.

O_3 simulations and observations from different stations are graphically and statistically compared in the Taylor diagram shown in **figure 10**. In this case, no large differences are observed; however, WRFu results show some improvement, according to metrics on **table XII.** Correlation coefficients vary from 0.76 to 0.89 for WRF and from 0.79 to 0.88 for WRFu. The index of agreement fluctuates between 0.67 and 0.85 in both experiments. Not only correlation values are high but also the index of agreement, even though RMSE and biases are high. Bias variability is 17.7 ppb for WRF and 17.2 ppb for WRFu; and RMSE variability is 11.4 and 13.7 ppb, respectively. The variability is obtained from the differences between maximum and minimum values highlighted in bold in each column.

Carbon monoxide

Highest observed CO values (above 2 ppm, with peak values up to 4 ppm) were obtained north of the city. In general, peak values are underestimated by simulations at all sites, except in CAM, where

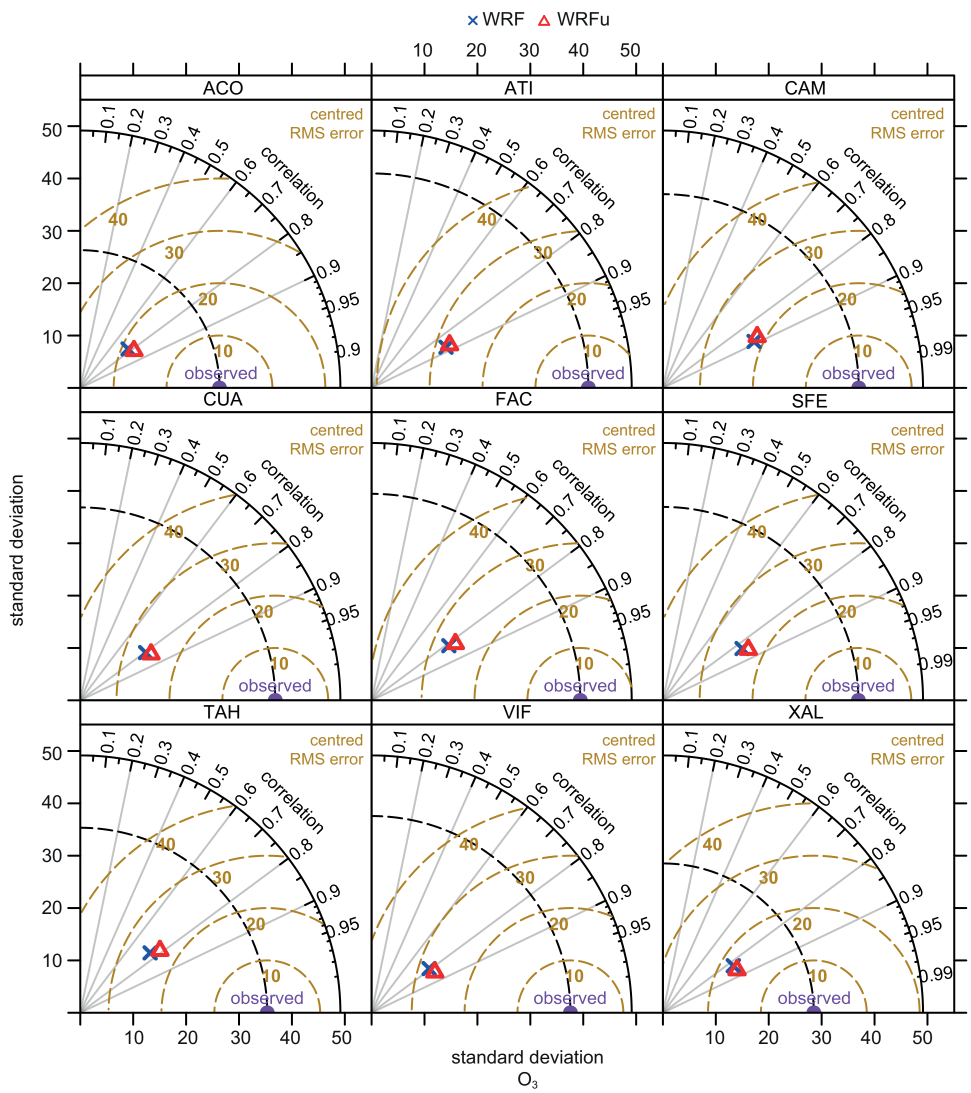

Fig. 10. Taylor diagrams of ozone (O_3) for different sites. The Weather Research and Forecasting (WRF) and Urban Weather Research and Forecasting (WRFu) simulations are graphically and statistically compared to a reference point in the *X* axis (observed), which corresponds to the monitoring station.

TABLE XII. VERIFICATION MEASURES FOR THE OZONE (O_3) BIAS ERROR: ROOT MEAN SQUARE ERROR (RMSE), CORRELATION COEFFICIENT AND INDEX OF AGREEMENT (I_a)* FOR THE WEATHER RESEARCH AND FORECASTING (WRF) AND URBAN WEATHER RESEARCH AND FORECASTING (WRFu) MODELS FOR DIFFERENT SITES.

O_3 Site	BIAS (ppb)		RMSE (ppb)		Correlation		I_a	
	WRF	WRFu	WRF	WRFu	WRF	WRFu	WRF	WRFu
ACO	–5.66	–8.41	19.57	19.49	0.77	0.82	0.72	0.75
CUA	**–12.36**	–14.72	28.81	28.99	0.8	0.83	0.7	0.71
FAC	–11.51	**–15.42**	29.2	30.11	0.81	0.83	0.74	0.74
ATI	–10.42	–13.21	**29.77**	**30.39**	0.88	0.87	0.73	0.73
CAM	2.33	–2.29	21.71	21.57	**0.89**	**0.88**	**0.85**	**0.85**
XAL	**5.37**	**1.79**	**18.4**	**16.68**	0.83	0.86	0.82	**0.85**
SFE	–10.54	–13.05	26.2	26.32	0.83	0.86	0.77	0.78
TAH	–7.75	–9.84	25.99	25.39	**0.76**	**0.79**	0.74	0.77
VIF	–7.41	–11.55	28.86	29.06	0.79	0.84	**0.67**	**0.69**

WRFu presented a higher peak than observations in day 23, suggesting an extreme episode of ambient CO concentrations north of the MCMA, since concentrations in WRFu and observations in stations ATI, FAC, VIF, and XAL also reproduced that behavior during the mentioned day, as observed in **figure 11**. It is also observed that CO ambient concentrations are larger in WRFu than in WRF at all sites. CO concentrations in the south region are lower in both observations and simulations, with values below 2 ppm, except for the rural station ACO located to the northeast, where observations are less than 1 ppm and simulations of WRF and WRFu present similar patterns with values near to 0 ppm, underestimating observations. This could suggest that the LCZ classification used for the simulation period better represent the local conditions of the urban area north of the MCMA, as compared to the south region and the rural site ACO. On the other hand, since local meteorological conditions change when using the urban parameterization, a revised emissions inventory must be used.

The diurnal variation in **figure 12** shows measured and simulated CO concentrations as average daily profiles of the nine sites compared in **figure 11**. This figure shows that, in general, WRFu simulations had a better performance when compared to observations, since peak values are better represented than in WRF simulations.

CO metrics are shown in **table XIII**. Bias variability is similar in both simulations when compared to observations; however, bias errors are lower in WRFu. Sites located north of the CDMX present larger reductions in bias with respect to WRF simulations. The bias error varies from –0.45 to 0.02 in WRFu and from 0.59 to –0.11 in WRF. RMSE values are also lower in WRFu than in WRF, except for CAM station, where RMSE increased in 24%. The RMSE for WRF was between 0.19-0.78 and between 0.16-0.66 for WRFu, with variabilities of 0.59 and 0.50 for WRF and WRFu, respectively. On the other hand, the correlation coefficient for WRF was from 0.19 to 0.75 and from 0.19 to 0.70 for WRFu, with an index of agreement from 0.38 to 0.50 for WRF and from 0.4 to 0.72 for WRFu. In this case, values obtained by WRFu were higher than those obtained by WRF when compared against observations, showing evidence of a better performance of the WRFu simulation when using urban parameterization with BEP.

The model performance evaluation for CO is represented by a Taylor diagram in **figure 13**, showing that WRFu simulations are closer to observations compared to WRF simulations.

For further explanation on the verification measures, please refer to section S1 in the supplementary material.

CONCLUSIONS

Using urban parameterization and FNL data reduces the bias error in temperature and bias variability. RMSE values are lower in most of the sites with WRFu simulations, reducing RMSE variability in 55% as compared to WRF simulations.

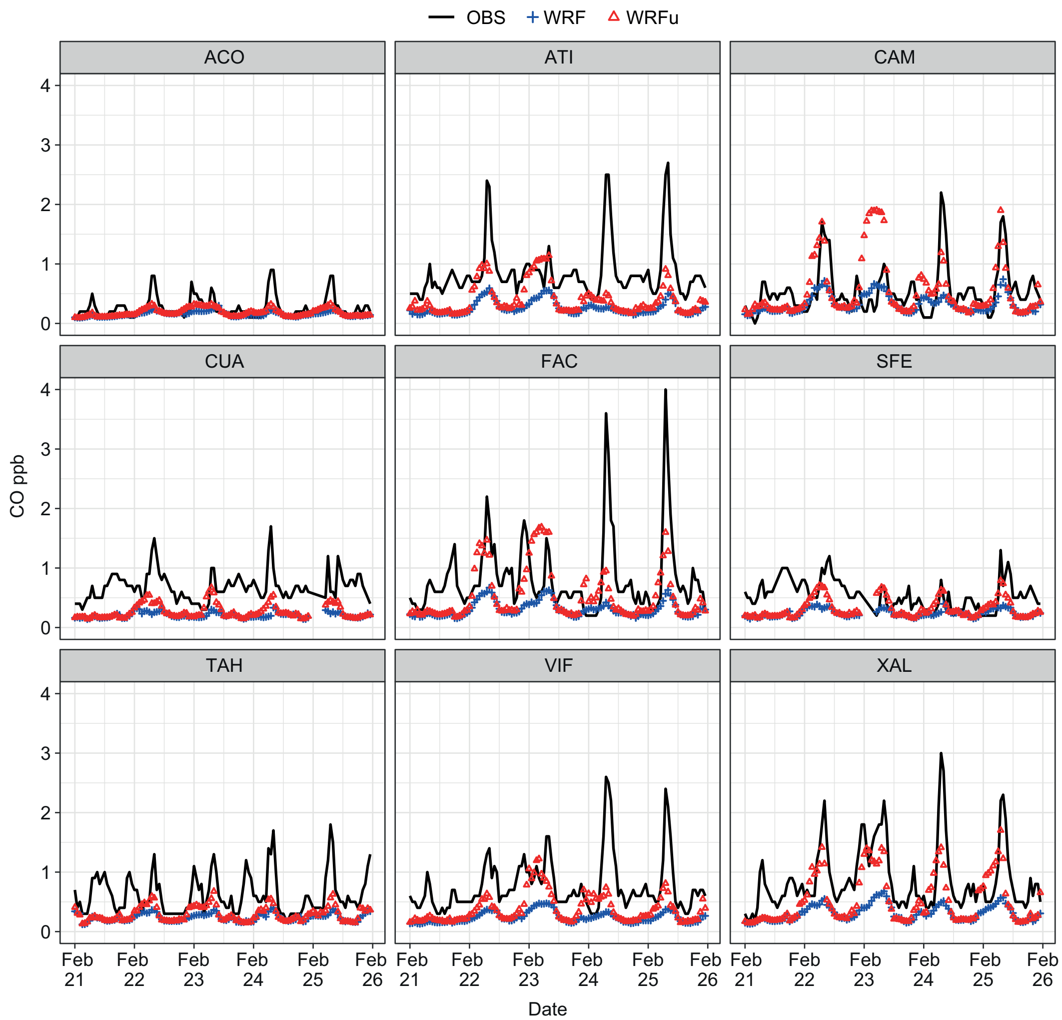

Fig. 11. Comparison of a carbon monoxide (CO) time series for different monitoring stations in Mexico City. Peak values of observations (OBS) are underestimated by simulations, although CO ambient concentrations are larger in Weather Research and Forecasting (WRF) simulations than in Urban Weather Research and Forecasting (WRFu) at all sites.

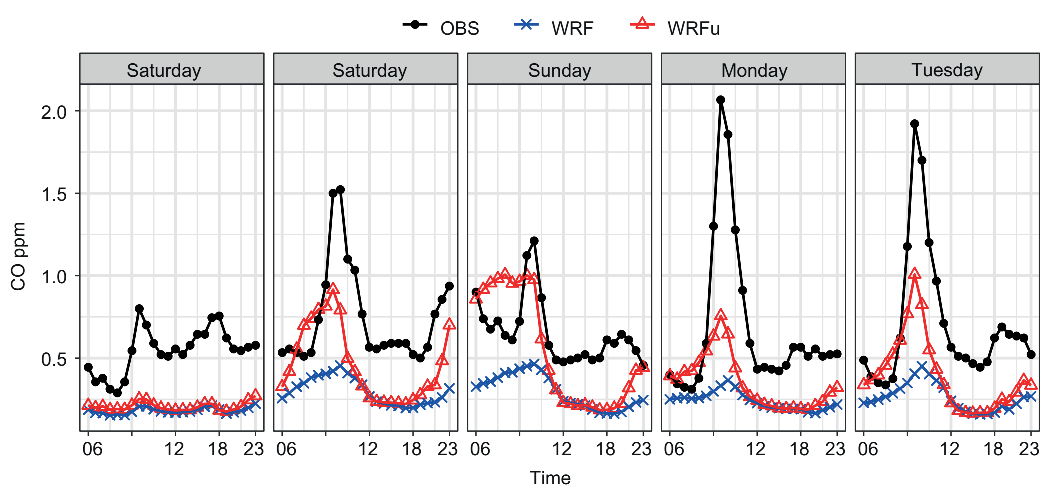

Fig. 12. Daily diurnal variation during the simulation period of carbon monoxide (CO) observations (OBS, in black), compared to Weather Research and Forecasting (WRF) and Urban Weather Research and Forecasting (WRFu) simulations.

TABLE XIII. VERIFICATION MEASURES FOR THE CARBON MONOXIDE (CO) BIAS ERROR: ROOT MEAN SQUARE ERROR (RMSE), CORRELATION COEFFICIENT AND INDEX OF AGREEMENT (I_a)* FOR THE WEATHER RESEARCH AND FORECASTING (WRF) AND URBAN WEATHER RESEARCH AND FORECASTING (WRFu) MODELS FOR DIFFERENT MONITORING SITES.

CO Site	BIAS (ppm)		RMSE (ppm)		Correlation		I_a	
	WRF	WRFu	WRF	WRFu	WRF	WRFu	WRF	WRFu
ACO	**–0.11**	–0.08	**0.19**	**0.16**	0.6	0.68	0.47	0.58
CUA	–0.48	–0.42	0.53	0.48	0.32	0.36	**0.38**	**0.4**
FAC	–0.52	–0.29	**0.78**	**0.66**	0.52	0.43	0.44	0.58
ATI	**–0.59**	**–0.45**	0.72	0.61	0.48	0.42	0.41	0.46
CAM	–0.22	**0.02**	0.41	0.51	0.52	0.38	0.5	0.62
XAL	–0.57	–0.34	0.73	0.52	**0.75**	**0.7**	**0.5**	**0.72**
SFE	–0.31	–0.24	0.39	0.36	**0.19**	**0.19**	0.44	0.46
TAH	–0.38	–0.33	0.49	0.43	0.55	0.56	0.48	0.52
VIF	–0.53	–0.39	0.66	0.55	0.6	0.52	0.46	0.52

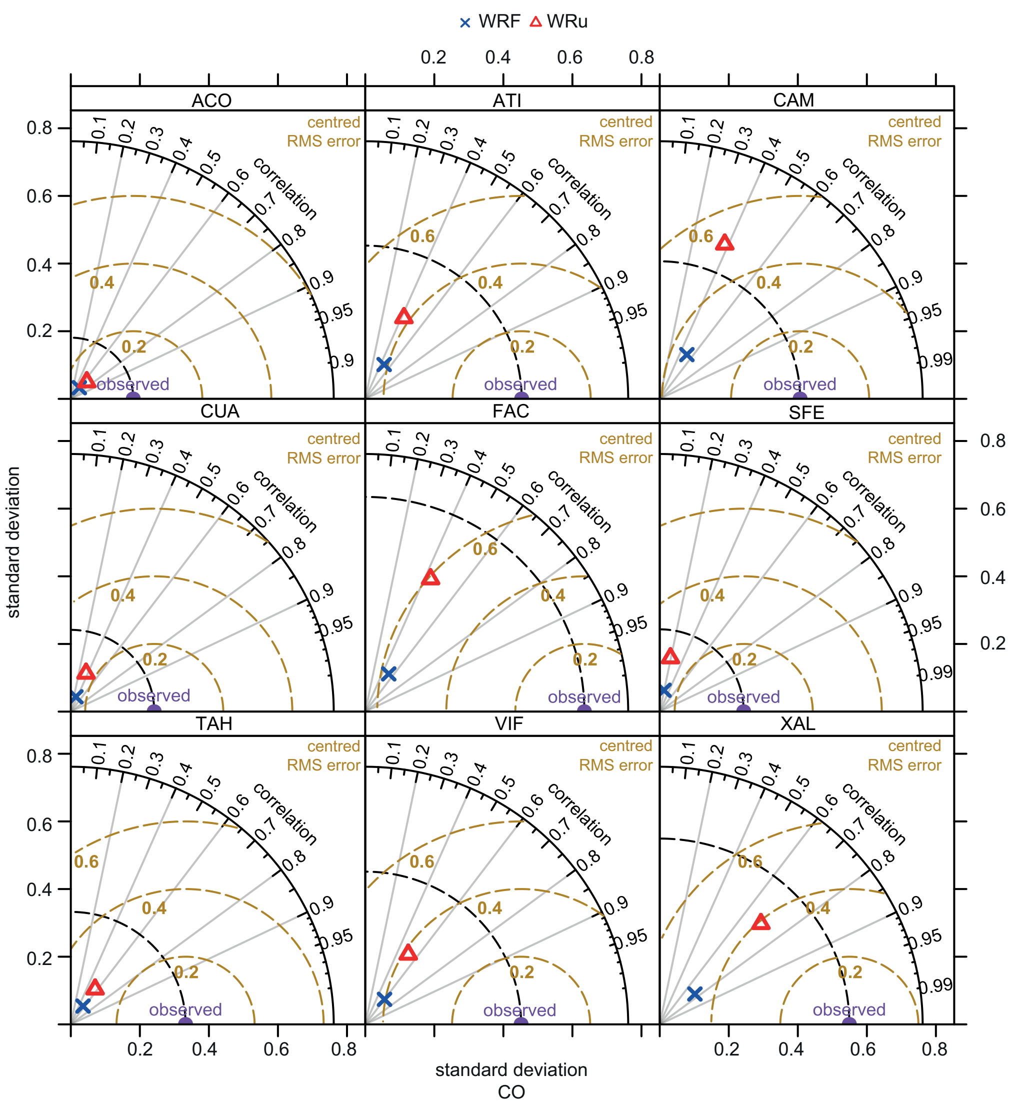

Fig. 13. Taylor diagram of carbon monoxide (CO) for different sites. Simulations of Weather Research and Forecasting (WRF) and Urban Weather Research and Forecasting (WRFu) simulations are compared to observations.

Correspondingly, WRFu simulations of temperature show a better agreement with observations even when these are underestimated, and peak values are reached in most of the sites. Nonetheless, in rural areas (ACO) and zones with low or moderate urbanization such as FAC, PED, SFE and TAH, observations of temperature tend to be lower than in urban areas. Observations of temperature often tend to be lower in non-urban areas compared to urban areas. This highlights the role of urban parameterization in improving simulations and increasing the accuracy of observations.

Increasing the resolution to 0.5 km in simulations has a positive impact in local weather since BIAS and RMSE are reduced and the correlation coefficient and index of agreement increase. WRFu temperature simulation at a 1-km grid resolution overestimates observations; however, bias variability and RMSE variability are reduced in 33 and 39%, respectively, when grid resolution is increased to 0.5 km and peak observation values are also reached, while WRF simulations tend to underestimate high values of temperature in both cases.

The highest CO concentrations are measured north of the MCMA, while lower values are measured south of the city, with the exception of the ACO rural site located northeast, which presented the lowest values. These patterns were reproduced by the WRFu-Chem model. Although simulations underestimate peak observation values at all sites, CO ambient concentrations are larger in WRFu-Chem than in WRF-Chem, indicating a less dilution rate and showing a better agreement with peak observation values. This suggests that the LCZ classification used for the simulation period better represents the urban area local conditions north of the MCMA than in the south and in the ACO rural site.

On the other hand, ozone simulations have differences in peak values. WRFu-Chem has slightly lower values than WRF-Chem. Peak observation values occurring during daylight are underestimated by simulations at all sites due to an increase in wind speed that reduces accumulation of O_3 precursors such as NO and VOC. In contrast, lower observation values during nighttime are overestimated, suggesting that simulated concentrations are influenced from O_3 regional transport. Bias and RMSE are relatively high; however, index of agreement values between 0.67 and 0.85 were obtained at all sites.

Improving the model performance in meteorological variables using urban parameterization with WRFu leads to a change in environmental concentrations. This experience deserves further investigation on local urban physical parameters and evaluation of emission inventories. Moreover, the LCZ classification used in this study should be actualized to improve local weather and reducing bias and RMSE errors to increase the WRFu-Chem model performance over the study area.

ACKNOWLEDGMENTS

The first author thanks the Consejo Nacional de Ciencia y Tecnología (CONACyT) for the financial support granted to carry out this research as part of his PhD studies. We also thank the support of the National High-Performance Computing Laboratory of the National Autonomous University of Mexico (LANCAD-UNAM) through project LANCAD-UNAM-DGTIC-179, and the Institute for Atmospheric Sciences and Climate Change (ICAyCC-UNAM).

REFERENCES

Bougeault P. and Lacarrère P. (1989). Parameterization of orography-induced turbulence in a mesobeta-scale model. Monthly Weather Review 117 (8), 1872-1890. https://doi.org/10.1175/1520-0493(1989)117<1872:POOITI>2.0.CO;2

Chen F. and Dudhia J. (2001). Coupling an advanced land surface-hydrology model with the Penn State-NCAR MM5 modeling system. Part I: Model implementation and sensitivity. Monthly Weather Review 129 (4), 569-585. https://doi.org/10.1175/1520-0493(2001)129%3C0569:CAALSH%3E2.0.CO;2

Chen F., Kusaka H., Bornstein R., Ching J., Grimmond C.S.B., Grossman-Clarke S., Loridan T., Manning K.W., Martilli A., Miao S., Sailor D., Salamanca F.P., Taha H., Tewari M., Wang X., Wyszogrodzki A.A. and Zhang C. (2011). The integrated WRF/urban modeling system: Development, evaluation, and applications to urban environmental problems. International Journal of Climatology 31 (2), 273-288. https://doi.org/10.1002/joc.2158

CONAGUA (2014). Resúmenes mensuales de temperaturas y lluvia. Comisión Nacional del Agua [online]. https://smn.conagua.gob.mx/es/climatologia/temperaturas-y-lluvias/resumenes-mensuales-de-temperaturas-y-lluvias 08/11/2019

Fast J.D., Gustafson W.I., Easter R.C., Zaveri R.A., Barnard J.C., Chapman E.G., Grell G.A. and Peckham S.E. (2006). Evolution of ozone, particulates, and aerosol direct radiative forcing in the vicinity of Houston using a fully coupled meteorology-chemistry-aerosol model. Journal of Geophysical Research: Atmospheres 111 (D21). https://doi.org/10.1029/2005JD006721

Fernández A.C. (2017). Influencia del cambio de la cobertura de suelo urbano en la meteorología de la Ciudad de México. M.Sc. Thesis. Centro de Ciencias de la Atmósfera, Universidad Nacional Autónoma de México, Mexico City, Mexico, 100 pp.

García-Reynoso J.A., Mar-Morales B.E. and Ruiz-Suárez L.G. (2018). Modelo de distribución espacial, temporal y de especiación del inventario de emisiones de México (año base 2008) para su uso en modelización de calidad del aire (DiETE). Revista Internacional de Contaminación Ambiental 34 (4), 635-649. https://doi.org/10.20937/RICA.2018.34.04.07

GCDMX (2019). Gobierno de la Ciudad del México. Calidad del aire: datos derivados del monitoreo atmosférico [online]. http://www.aire.cdmx.gob.mx/ 06/08/2019

Grell G.A., Peckham, S.E. Schmitz R., McKeen S.A., Frost G., Skamarock W.C. and Eder B. (2005). Fully coupled online chemistry within the WRF model. Atmospheric Environment 39 (37), 6957-6975. https://doi.org/10.1016/j.atmosenv.2005.04.027

INECC (2017). Preparación de un inventario de emisiones para modelación Report.. Instituto Nacional de Ecología y Cambio Climático, Mexico City, Mexico, 27 pp.

INEGI (2018). Marco Geoestadístico Nacional. Instituto Nacional de Estadística y Geografía [online]. https://www.inegi.org.mx/temas/mg/ 15/11/2022

INEGI (2022). Cuéntame de México. Instituto Nacional de Estadística y Geografía [online]. https://cuentame.inegi.org.mx/monografias/informacion/df/territorio/relieve.aspx?tema=me&e=09 15/11/2022

Janjić Z.I. (1994). The step-mountain Eta coordinate model: Further developments of the convection, viscous sublayer, and turbulence closure schemes. Monthly Weather Review 122 (5), 927-945. https://doi.org/10.1175/1520-0493(1994)122<0927:TSMECM>2.0.CO;2

Kong J., Zhao Y., Carmeliet J. and Lei C. (2021). Urban heat island and its interaction with heatwaves: A review of studies on mesoscale. Sustainability 13 (19), 10923. https://doi.org/10.3390/su131910923

Lei W., Zavala M., de Foy B., Volkamer R. and Molina L.T. (2008). Characterizing ozone production and response under different meteorological conditions in Mexico City. Atmospheric Chemistry and Physics 8 (24), 7571-7581. https://doi.org/10.5194/acp-8-7571-2008

Liao J., Wang T., Wang X., Xie M., Jiang Z., Huang X. and Zhu J. (2014). Impacts of different urban canopy schemes in WRF/Chem on regional climate and air quality in Yangtze River Delta, China. Atmospheric Research 145-146, 226-243. http://dx.doi.org/10.1016/j.atmosres.2014.04.005

Martilli A., Clappier A. and Rotach W.M. (2002). An urban surface exchange parameterisation for mesoscale models. Boundary-Layer Meteorology 104, 261-304. https://doi.org/10.1023/A:1016099921195

Martilli A., Brousse O. and Ching J. (2016). Urbanized WRF modeling using WUDAPT [online]. http://www.wudapt.org/wp-content/uploads/2016/05/Urbanized-WRF-modeling-using-WUDAPT-web-version-March2016.pdf 14/11/2022

Mlawer E.J., Taubman S.J., Brown P.D., Iacono M.J. and Clough S.A. (1997). Radiative transfer for inhomogeneous atmospheres: RRTM, a validated correlated k model for the longwave. Journal of Geophysical Research: Atmospheres 102 (D14), 16663-16682. https://doi.org/10.1029/97JD00237

NCAR (2020a). WRF-Chem model. National Center for Atmospheric Research [online]. https://www2.acom.ucar.edu/wrf-chem 15/11/2022

NCAR (2020b). NCEP FNL operational model global tropospheric analyses, continuing from July 1999. Research Data Archive at the Computational and Information Systems Laboratory, National Center for Atmospheric Research [online]. https://rda.ucar.edu/datasets/ds083.2/ 13/08/2020

NCAR (2020c). NCEP North American Mesoscale (NAM) 12 km analysis. Research Data Archive at the Computational and Information Systems Laboratory, National Center for Atmospheric Research [online]. https://rda.ucar.edu/datasets/ds609.0/ 30/01/2020

Noyola M. (2014). Estudio de monitoreo de la calidad del aire en Bosques de Santa Fe, Cuajimalpa, D.F., del 19 al 26 de febrero de 2014. Report. Dirección General de Investigación sobre la Contaminación Urbana y Regional, Instituto Nacional de Ecología y Cambio Climático. Mexico City, Mexico, 13 pp.

Peckham S., Grell G.A., McKeen S.A., Wiedinmyer C., Fast J.D., Gustafson W.I., Ghan S.J., Zaveri R., Easter R.C., Barnard J., Chapman E., Schmitz R., Salzmann M. and Freitas S. (2010). WRF-Chem version 3.2 user's guide. Manual. National Oceanic and Atmospheric Administration. Boulder, CO, USA, 87 pp.

Qian Y., Gustafson W. I. and Fast J.D. (2010). An investigation of the sub-grid variability of trace gases and aerosols for global climate modeling. Atmospheric Chemistry and Physics 10 (14), 6917-6946. https://doi.org/10.5194/acp-10-6917-2010

Ribeiro I., Martilli A., Falls M., Zonato A. and Villalba G. (2021). Highly resolved WRF-BEP/BEM simulations over Barcelona urban area with LCZ. Atmospheric Research 248, 105220. https://doi.org/10.1016/j.atmosres.2020.105220

Santiago J.L. and Martilli A. (2010). A dynamic urban canopy parameterization for mesoscale models based on computational fluid dynamics Reynolds-averaged Navier-Stokes microscale simulations. Boundary-Layer Meteorology 137, 417-439. https://doi.org/10.1007/s10546-010-9538-4

SEDEMA (2017). Calidad del aire en la Ciudad de México. Informe 2016. Report. Dirección General de Gestión de la Calidad del Aire, Dirección de Monitoreo Atmosférico. Secretaría del Medio Ambiente de la Ciudad de México, Mexico City, Mexico, 204 pp.

SEDATU (2018). Delimitación de zonas metropolitanas de México 2015. Report. Secretaría de Desarrollo Agrario, Territorial y Urbano. Mexico City, Mexico, 286 pp.

SEDEMA (2019). Aviso por el que se da a conocer el programa para prevenir y responder a contingencias ambientales atmosféricas en la Ciudad de México. Secretaría del Medio Ambiente de la Ciudad de México. Gaceta Oficial de la Ciudad de México, 28 de mayo. Mexico City, Mexico, 24 pp.

Skamarock W.C., Klemp J.B., Dudhia J., Gill D.O., Barker D.M., Wang W. and Powers J.G. (2005). A description of the advanced research WRF version 2. Technical note (No. NCAR/TN-468+STR). University Corporation for Atmospheric Research. Boulder, CO. USA, 88 pp. http://dx.doi.org/10.5065/D6DZ069T

Stewart I.D. and Oke T.R. (2012). Local climate zones for urban temperatures studies. Bulletin of the American Meteorological Society 93 (12), 1879-1900. https://doi.org/10.1175/BAMS-D-11-00019.1

Stewart I.D., Oke T.R. and Scott K.E. (2014). Evaluation of the 'local climate zone' scheme using temperature observations and model simulations. International Journal of Climatology 34 (4), 1062-1080. https://doi.org/10.1002/joc.3746

Stockwell W.R., Middleton P., Chang J.S. and Tang X. (1990). The second-generation regional acid deposition model chemical mechanism for regional air quality modeling. Journal of Geographical Research: Atmospheres 95 (D10), 16343-16367. https://doi.org/10.1029/JD095iD10p16343

Tewari M., Chen F., Kusaka H. and Miao S. (2007). Coupled WRF/Unified Noah/Urban-Canopy modeling system. National Center for Atmospheric Research [online]. https://ral.ucar.edu/sites/default/files/public/product-tool/WRF-LSM-Urban.pdf 14/11/2022

Tie X., Madronich S., Li G., Ying Z., Weinheimer A., Apel E. and Campos T. (2009). Simulation of Mexico City plumes during the MIRAGE-Mex field campaign using the WRF-Chem model. Atmospheric Chemistry and Physics 9 (14), 4621-4638. https://doi.org/10.5194/acp-9-4621-2009

Tie X., Brasseur G. and Ying Z. (2010). Impact of model resolution on chemical ozone formation in Mexico City: Application of the WRF-Chem model. Atmospheric Chemistry and Physics 10 (18), 8983-8995. https://doi.org/10.5194/acp-10-8983-2010

Ulpiani G. (2021) On the linkage between urban heat island and urban pollution island: Three-decade literature review towards a conceptual framework. Science of The Total Environment 751, 141727. https://doi.org/10.1016/j.scitotenv.2020.141727

UN (2019). World urbanization prospects: The 2018 revision. Report ST/ESA/SER.A/420. Department of Economic and Social Affairs, Population Division, United Nations. New York, USA, 103 pp.

Wilks D.S. (2006). Statistical methods in the atmospheric sciences. 2nd ed. Academic Press. San Diego, California, USA, 627 pp.

Willmott C.J. (1982). Some comments on the evaluation of model performance. Bulletin of the American Meteorological Society 63 (11), 1309-1313. https://doi.org/10.1175/1520-0477(1982)063<1309:SCOTEO>2.0.CO;2

Wong C.H.H., Cai M., Ren C., Huang Y., Liao C. and Yin S. (2021). Modelling building energy use at urban scale: A review on their account for the urban environment. Building and Environment 205, 108235. https://doi.org/10.1016/j.buildenv.2021.108235

Zhang Y., Dubey M.K., Olsen S.C., Zheng J. and Zhang R. (2009). Comparisons of WRF/Chem simulations in Mexico City with ground-based RAMA measurements during the 2006-MILAGRO. Atmospheric Chemistry and Physics 9 (11), 3777-3798. https://doi.org/10.5194/acp-9-3777-2009

SUPPLEMENTARY MATERIAL

S1. Verification measures

To compare the model with observations or other modeling experiments, the index of agreement (I_a), the mean error (ME) or bias, the root mean square error (RMSE), and the Pearson correlation coefficient (R) were used to assess model performance. These metrics are briefly described below, where P_i represents i_{th} predicted value and O_i represents de i_{th} observed value of n total pair of observations and simulations.

I_a is defined in equation 1. Its possible range is $0 \leq I_a \leq 1$, where $I_a = 1$ suggests a perfect agreement between forecast and observations, and $I_a = 0$ denotes that there is no agreement between the data pair of forecast and observations (Willmott 1982).

$$I_a = 1 - \left[\frac{\sum_{i=1}^{n} \left(P_i - O_i\right)^2}{\sum_{i=1}^{n} \left(\left|P_i - \bar{O}\right| + \left|O_i - \bar{O}\right| \right)^2} \right] \tag{1}$$

ME is the difference between the average forecast and average observation and is defined in equation 2. In particular, ME is equal to the bias and expresses the bias of forecasts. When these are too high on average, they will exhibit ME > 0 and forecasts that are too low on average will exhibit ME < 0. ME = 0 denotes a perfect forecast (Wilks 2006).

$$ME = BIAS = \frac{1}{n} \sum_{i=1}^{n} P_i - O_i \tag{2}$$

R (equation 3) measures the relationship between two variables. It is bounded by −1 and 1, that is, $-1 \leq R \leq 1$. If R = −1 there is a perfect, but negative linear association between observations and forecast. Similarly, if R = 1 there is a perfect positive linear association between observations and modeled values. On the contrary, a correlation coefficient = 0 means that there is no linear relationship between the variables (Wilks 2006).

$$Corr = R = \frac{1}{n-1} \sum_{i=1}^{n} \frac{(P_i - \bar{P})}{\delta_p} \frac{(O - \bar{O})}{\delta_o} \tag{3}$$

where δ_o and δ_p are the standard deviations of observations and modeled values, respectively (Wilks 2006), defined as:

$$\delta_O = \left[\frac{1}{n-1} \sum_{i=1}^{n} \left(O_i - \bar{O}\right)^2 \right]^{\frac{1}{2}}, \ \delta_p = \left[\frac{1}{n-1} \sum_{i=1}^{n} \left(P_i - \bar{P}\right)^2 \right]^{\frac{1}{2}} \tag{4}$$

The RMSE provides a typical magnitude for modeling error and a good overall measure of how close the modeled values are to observed values. A perfect forecast has RMSE = 0. Equation 5 is easy to interpret since it preserves the same physical dimensions of the variables (Willmott 1982).

$$RMSE = \left[\frac{1}{n} \sum_{i=1}^{n} (P_i - O_i)^2 \right]^{\frac{1}{2}} \tag{5}$$

The Taylor diagrams in figures 6, 7, 10 and 13, show in a 2D plot the model evaluation performance of several experiments at a time, indicating the most realistic. It uses three statistics simultaneously: the Pearson correlation coefficient (R, equation 3), the standard deviation (equation 4), and the root-mean-square error (RMSE, equation 5).